Research

New Phytologist

AIM1-dependent high basal salicylic acid accumulation modulates stomatal aperture in rice

Lei Xu[1]*, Hongyu Zhao[1]*, Junbin Wang[2,3]*, Xuming Wang[4], Xianqing Jia[1], Long Wang[1], Zhuang Xu[1], Ruili Li[1], Kun Jiang[5,6], Zhixiang Chen[7], Jie Luo[8], Xiaodong Xie[2] and Keke Yi[1]

[1]State Key Laboratory of Efficient Utilization of Arid and Semi-arid Arable Land in Northern China, Institute of Agricultural Resources and Regional Planning, Chinese Academy of Agricultural Sciences, Beijing 100081, China; [2]International Joint Center for the Mechanismic Dissection and Genetic Improvement of Crop Stress Tolerance, College of Agriculture & Resources and Environmental Sciences, Tianjin Agricultural University, Tianjin 300392, China; [3]College of Basic Sciences, Tianjin Agricultural University, Tianjin 300392, China; [4]State Key Laboratory for Managing Biotic and Chemical Threats to the Quality and Safety of Agro-Products, Ministry of Agriculture Key Laboratory for Plant Protection and Biotechnology, Zhejiang Provincial Key Laboratory of Plant Virology, Zhejiang Academy of Agricultural Sciences, Hangzhou 310021, China; [5]College of Life Sciences, Zhejiang University, Hangzhou, Zhejiang 310058, China; [6]College of Life Sciences, China Jiliang University, 258 Xueyuan Street, Hangzhou, Zhejiang 310018, China; [7]Purdue Center for Plant Biology, Department of Botany and Plant Pathology, Purdue University, 915 W. State Street, West Lafayette, IN 47907-2054, USA; [8]Sanya Nanfan Research Institute of Hainan University, Hainan Yazhou Bay Seed Laboratory, Sanya 572025, China

Authors for correspondence:
Keke Yi
Email: yikeke@gmail.com

Xiaodong Xie
Email: xiex@tjau.edu.cn

Jie Luo
Email: jie.luo@hainanu.edu.cn

Received: *7 September 2022*
Accepted: *18 February 2023*

New Phytologist (2023) **238:** 1420–1430
doi: 10.1111/nph.18842

Key words: OsAIM1, rice, salicylic acid biosynthesis, shoot temperature, stomata.

Summary

- The basal levels of salicylic acid (SA) vary dramatically among plant species. In the shoot, for example, rice contains almost 100 times higher SA levels than Arabidopsis. Despite its high basal levels, neither the biosynthetic pathway nor the biological functions of SA are well understood in rice.
- Combining with metabolite analysis, physiological, and genetic approaches, we found that the synthesis of basal SA in rice shoot is dependent on *OsAIM1*, which encodes a beta-oxidation enzyme in the phenylalanine ammonia-lyase (PAL) pathway.
- Compromised SA accumulation in the *Osaim1* mutant led to a lower shoot temperature than wild-type plants. However, this shoot temperature defect resulted from increased transpiration due to elevated steady-state stomatal aperture in the mutant. Furthermore, the high basal SA level is required for sustained expression of *OsWRKY45* to modulate the steady-state stomatal aperture and shoot temperature in rice.
- Taken together, these results provide the direct genetic evidence for the critical role of the PAL pathway in the biosynthesis of high basal level SA in rice, which plays an important role in the regulation of steady-state stomatal aperture to promote fitness under stress conditions.

Introduction

Salicylic acid (SA) is an important plant hormone that regulates growth, development, and various stress responses (Rivas-San Vicente & Plasencia, 2011). The best-established role of SA is the regulation of plant defense response against pathogen infection. The earliest report of SA in plant defense is the effect of exogenously applied SA in protecting tobacco leaves against viral infection (White, 1979). Subsequently, it was found that SA could act as an endogenous signal in plant defense (Raskin, 1992). During the past 30 yr or so, extensive progress has been made in the understanding of the signaling pathway of SA-mediated defense response in plants. In addition to its role in plant defense, SA plays important roles in root growth, leaf senescence, and heat production in some thermogenic plants (Zhang *et al.*, 2013; Tan *et al.*, 2020).

Endogenous SA is involved in thermogenesis in arum lily flowers for dispersing flower odor to attract pollinators (Raskin *et al.*, 1987). The SA levels in the flowers of the thermogenic plants surge *c.* 100-fold upon blooming, leading to a temperature increase of *c.* 10°C above the ambient temperature. Increased levels of SA promote thermogenesis by inducing the expression of genes encoding alternative oxidase (AOX), a key enzyme in the alternative respiratory pathway in mitochondria that is uncoupled from ATP production and releases energy as heat (Raskin *et al.*, 1989; Rhoads & McIntosh, 1992). In most plants, basal SA levels are very low SA (*c.* 100 ng g^{-1} fresh weight (FW)), but they can increase drastically in lily flowers during development or under certain biotic and abiotic stress conditions. Other plants such as Populus and rice have very high basal SA levels (>10 μg g^{-1} FW) under normal growth conditions. Whether basal SA contributes to thermogenesis in non-thermogenic plants, especially those with high basal SA levels, is unknown.

*These authors contributed equally to this work.

Salicylic acid is synthesized through two distinct pathways in plants: the isochorismate synthase (ICS) pathway and the phenylalanine ammonia-lyase (PAL) pathway (Dempsey *et al.*, 2011). Chorismate is a precursor of both these pathways. Isochorismate synthase catalyzes chorismite to isochorismate in the plastid. Isochorismate is exported by ENHANCED DISEASE SUSCEPTIBILITY5 (EDS5) to the cytosol, where the cytosolic amidotransferase avrPphB SUSCEPTIBLE3 (PBS3) catalyzes the conjugation of glutamate to isochorismate to produce isochorismate-9-glutamate, which spontaneously decomposes into SA and 2-hydroxy-acryloyl-*N*-glutamate (Rekhter *et al.*, 2019). On the other hand, PAL catalyzes the chorismate-derived L-phenylalanine into cinnamic acid (CA), which is then converted to SA via o-coumarate or benzoic acid (BA). β-oxidation plays a crucial role in conversion of o-coumarate to SA or CA to benzoate (Dempsey *et al.*, 2011).

The PAL and ICS biosynthetic routes contribute differently to the biosynthesis of SA in different plant species. *Arabidopsis* contains low basal levels of SA, and most of defense-related SA is synthesized via the ICS pathway (Wildermuth *et al.*, 2001; Garcion *et al.*, 2008). A more recent study has shown that ABNORMAL INFLOURESCENCE MERISTEM 1 (AIM1), a peroxisome β-oxidation enzyme, functions in SA biosynthesis in Arabidopsis seeds (Bussell *et al.*, 2014), indicating a role for the AIM1-dependent β-oxidation functions in the PAL pathway in basal SA biosynthesis. In Populus, the single ICS-encoding gene primarily functions in phylloquinone biosynthesis and SA is synthesized from CA via the PAL pathway (Yuan *et al.*, 2009; Xue *et al.*, 2013). In soybean, the PAL and ICS pathways are equally important for pathogen-induced SA biosynthesis (Shine *et al.*, 2016). Rice contains a very high basal level of SA, two orders of magnitude higher than *Arabidopsis* (Silverman *et al.*, 1995). However, the contribution of the two biosynthesis pathways to the high basal SA level is not well understood in rice. Early feeding studies suggested that rice shoot converted CA and BA into SA (Silverman *et al.*, 1995). In a previous study, we found that the OsAIM1-dependent PAL pathway is important for SA synthesis in rice roots (Xu *et al.*, 2017). Rice shoots contain a much higher level of SA than the roots (Pal *et al.*, 2014). Although a previous study has implicated ICS in rice SA production (Choi *et al.*, 2015), there has been no genetic evidence for how the basal SA is produced in rice shoots.

Although rice is well known to contain a higher basal level of SA, its biological function is less clear. Unlike in Arabidopsis, SA levels do not greatly increase after pathogen infection in rice (Silverman *et al.*, 1995). However, several studies have suggested that SA plays a role in defense against pathogen infection in rice (Shimono *et al.*, 2007; Kouzai *et al.*, 2018; Jiang *et al.*, 2020). It has been suggested that SA is important for protecting rice from oxidative damage during pathogen infections (Yang *et al.*, 2004). In addition, we have previously shown that SA is crucial for meristem activity in rice roots (Xu *et al.*, 2017), but it is still largely unclear about the biological function of high basal levels of SA in rice shoots.

In this study, we have found that the high basal SA level is unaltered in a rice knockout mutant for its sole ICS gene. By contrast, the mutant for OsAIM1 is drastically reduced in basal SA levels in the rice shoots. These results provide the first genetic evidence for the PAL pathway in the biosynthesis of high basal SA levels in rice. In addition, we have also found that the high basal level of SA in rice shoots is required for maintaining the steady-state stomatal aperture and shoot temperature through a pathway that is dependent on the rice OsWRKY45 transcription factor. We have further shown that the high basal SA levels are important for tolerance to abiotic stresses in rice.

Materials and Methods

Plant materials and growth conditions

Hydroponic experiments were conducted using a modified rice (*Oryza sativa* L.) culture solution containing 1.425 mM NH_4NO_3, 0.2 mM NaH_2PO_4, 0.513 mM K_2SO_4, 0.998 mM $CaCl_2$, 1.643 mM $MgSO_4$, 0.009 mM $MnCl_2$, 0.075 mM $(NH_4)_6Mo_7O_{24}$, 0.019 mM H_3BO_3, 0.155 mM $CuSO_4$, and 0.152 mM $ZnSO_4$ with 0.125 mM EDTA-Fe. pH of the solution was adjusted to 5.5. All the plants were grown in a glasshouse with a 12 h : 12 h, 30°C : 22°C, day : night photoperiod, *c.* 200 μmol m^{-2} s^{-1} photon density, and *c.* 60% humidity.

For *Xanthomonas oryzae* pv *Oryzae* (*Xoo*) infection, *Xoo* strain PXO 341 was cultured in modified Wakimoto's medium (per liter: peptone, 5 g; sucrose, 20 g; $MgSO_4{\cdot}7H_2O$, 0.25 g; K_2HPO_4, 0.5 g; pH 7.2–7.4) at 28°C. Fourteen-day-old rice seedlings were treated with water or *Xoo* for 24 h, then the shoot was sampled for SA quantification and gene expression analysis.

For measurement of stomatal conductance after H_2O_2 treatment, 21-d-old seedlings were sprayed with 0.5 mM H_2O_2 for 2 h.

For measurement of H_2O_2 level and stomatal conductance after NaCl or polyethylene glycol (PEG) treatment, 21-d-old seedlings were treated with 100 mM NaCl/20% PEG and 100 mM NaCl/20% PEG+ 200 μM SA (SA was added before NaCl/PEG treatment for 3 h) for 6 h.

Plasmid construction and plant transformation

The sequence information for primers used to construct vectors is shown in Supporting Information Table S1. For *ProOsWRKY45:GUS* vector, the 2753 bp promoter before the start code was introduced into the PstI and KpnI sites on pCAMBIA 1300-GUS vector. For *ProNPR1:GUS* vector, the 2425 bp promoter before the start code was introduced into the SalI and KpnI sites on pCAMBIA 1300-GUS vector. For *ProOsWRKY45:OsWRKY45* vector, the 4428 bp genome fragment was introduced into the KpnI and XbaI sites on pCAMBIA 1300 vector. The constructs were transformed into mature embryos developed from seeds of wild-type (WT; 'Shishoubaimao') or the *Oswrky45* mutant via *Agrobacterium tumefaciens* mediated transformation. The primers used are listed in Table S1.

Histochemical localization of GUS expression

For GUS staining, the tissues were incubated in a solution containing 50 mM sodium phosphate buffer (pH 7.0), 5 mM K3Fe

(CN)6, 5 mM K4Fe(CN)6, 0.1% Triton X-100, and 1 mM X-Gluc at 37°C. Sections (35 μm) of various plant tissues were made by vibratome (Leica VT 1000 S; Leica Biosystems, Nussloch, Germany). Images were taken by microscope (Nikon Eclipse Ni; Tokyo, Japan).

Quantitative RT-PCR

Reverse transcription was performed using 2 μg of total RNA and M-MuLV Reverse Transcriptase (NEB) according to the manufacturer's instructions. Quantitative PCR (qPCR) was performed using the Roche SYBR green I kit on the LightCycler480 machine (Roche Diagnostics, Basel, Switzerland) according to the manufacturer's instructions. Three biological replicates were performed for each gene. Rice *Actin* gene was used as an internal control. The primers used are listed in Table S1.

NBT and HPF staining

Rice roots were stained for 30 min in a solution of 2 mM nitroblue tetrazolium (NBT) or 5 μM 3′-(p-hydroxyphenyl) fluorescein (HPF) in 20 mM phosphate buffer (pH 6.1). The reaction was stopped by transferring the seedlings to distilled water. Root tips were imaged under bright-field illumination for NBT staining or GFP channel for HPF staining on a Nikon microscope. The intensity of NBT and HPF staining was quantified using ImageJ software.

Metabolites measurement

For metabolites measurements, seedlings were grown in a cultural solution for 2 wk. The aerial parts and roots were separately collected and freeze-dried. The freeze-dried tissues were used for metabolites measurement, following previously published methods (Chen *et al.*, 2013). The sample extracts were analyzed using an LC–ESI–MS/MS system (HPLC, Shim-pack UFLC Shimadzu CBM20A system, www.shimadzu.com; MS, Applied Biosystems 4000 Q TRAP, www.appliedbiosystems.com).

Stomatal aperture measurement

For imaging rice stomata, leaves of 3-wk-old plants were fixed with 2.5% (v/v) glutaraldehyde, and stomatal pictures were obtained by a Hitachi TM3030Plus scanning electron microscopy. At least 60 stomata were examined in each line, and the assays were repeated three times.

Measurements of water loss

Water loss rates of the detached leaves from 3-wk-old plants were measured by monitoring the FW loss at indicated points under a constant temperature (28°C) and humidity (60%). The percentage loss of weight was calculated based on the initial weight of the plants.

Thermal imaging

Thermal images of the plant were taken with an infrared thermal camera (FLIR T400; FLIR Systems, Boston, MA, USA) and were subsequently analyzed through the FLIR R&D software.

Gas exchange measurements

The stomatal conductance (Gs) and transpiration rate (E) were measured using a LI-6800 portable photosynthesis system (PP Systems, Lincoln, NE, USA) at 28°C, 200 μmol m^{-2} s^{-1} light, 400 μmol mol^{-1} CO_2, and 60% relative humidity.

Results

OsAIM1 but not OsICS is required for high basal SA accumulation in rice shoot

In plants, SA is synthesized through the ICS pathway and the PAL pathway (Fig. 1a). *Arabidopsis* contains low basal levels of SA and synthesizes defense-related SA mostly via the ICS pathway. Rice contains much higher levels of SA in shoots but the pathway responsible for rice SA synthesis has not been genetically established. Rice genome contains a single copy *ICS* gene (Yuan *et al.*, 2009). To determine whether the ICS pathway participates in SA biosynthesis in rice shoots, we have isolated and analyzed an *Osics1* mutant (PFG_3A-08161.R) from the T-DNA insertion mutant library (Fig. S1a). The mutant was confirmed by PCR-based DNA genotyping using primers flanking the T-DNA insertion site (Fig. S1b). The failure to detect the expression of *OsICS1* suggested that *Osics1* is a null mutant (Fig. S1c). Notably, the SA content in the *Osics1* mutant is similar to that in WT (Fig. 1b). This result indicates that OsICS1 is not required for high basal levels of SA production in rice shoots.

It has been reported that the ICS1 is essential for phylloquinone other than the SA biosynthesis in barley. The *ics1* mutant displays comparable SA content with the WT plants, while the deficiency of phylloquinone in the mutant leads to a wilting symptom (Qin *et al.*, 2019). Likewise, *Osics1* mutant displayed a pale green to yellowish pigmentation in leaf and started wilting *c.* 10 d after germination (Fig. S1d,e), implying that OsICS1 might be required for phylloquinone other than SA biosynthesis.

In a previous study, we found that OsAIM1-dependent β-oxidation is required for SA biosynthesis in rice roots and OsAIM1 is also strongly expressed in rice shoots (Xu *et al.*, 2017). Therefore, OsAIM1 might also participate in SA synthesis in rice shoots. To test this possibility, we measured the shoot SA content in the *Osaim1* mutant. As shown in Fig. 1c, the SA content in the mutant shoots was only *c.* 10% of that in WT shoots. The introduction of the *OsAIM1* gene driven by either its native promoter or the *CaMV 35S* promoter fully restores the SA content of the mutant to the WT levels (Fig. 1c). Thus, the OsAIM1-dependent β-oxidation is also required for the high basal levels of SA accumulation in rice shoots.

In the PAL pathway, β-oxidation is required for the shortening of the side chain of CA to produce BA, which is then converted

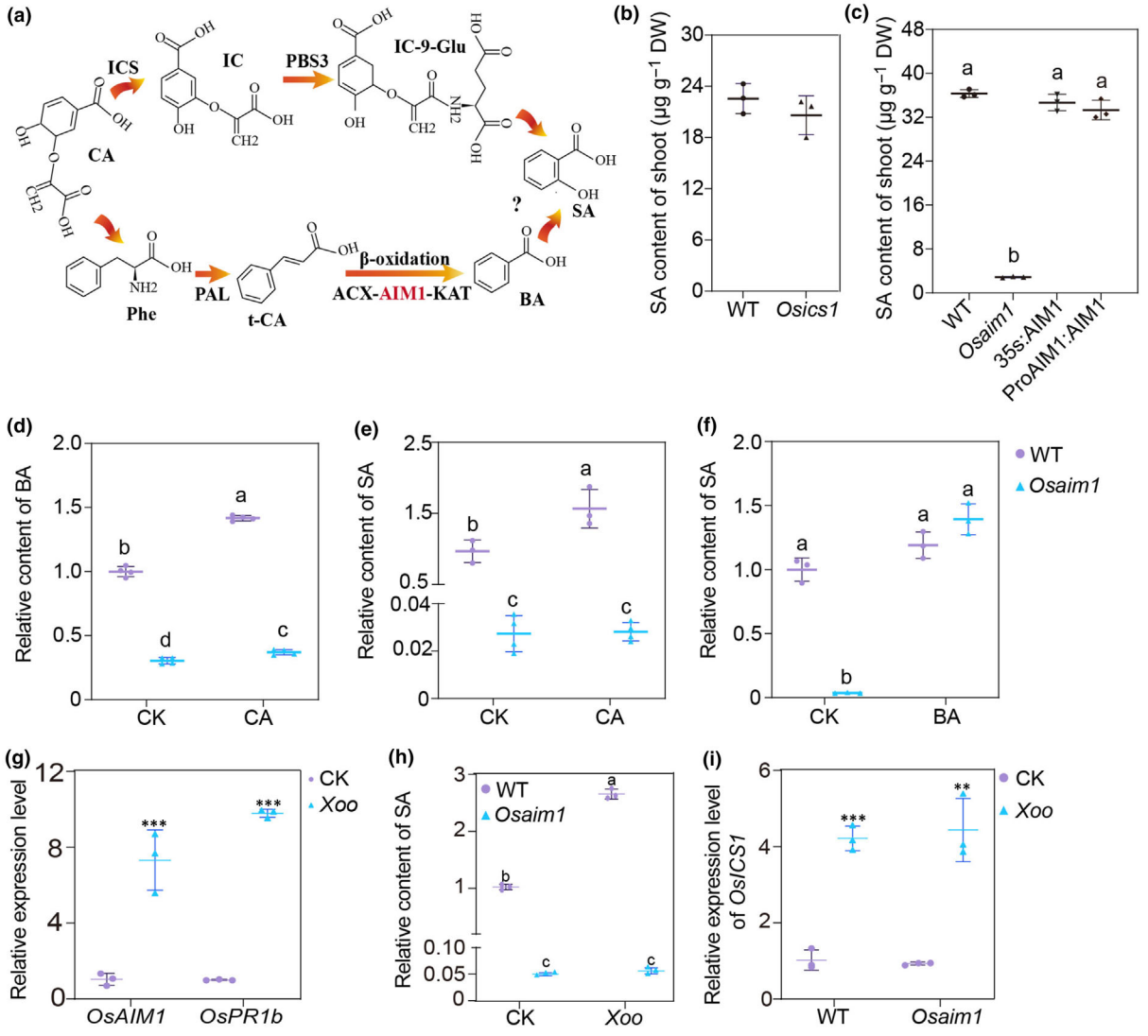

Fig. 1 OsAIM1 is essential for salicylic acid (SA) biosynthesis in rice shoots. (a) The biosynthetic pathways for SA. ACX, acyl-CoA oxidase; BA, benzoic acid; CA, chorismite; IC, isochorismate; IC-9-Glu, IC-9-glutamate; ICS, isochorismate synthase; KAT, L-3-ketoacyl-CoA thiolase; PAL, phenylalanine ammonia lyase; PBS3, avrPphB susceptible 3; Phe, phenylalanine; t-CA, trans-cinnamic acid; ? represents the gene for BA to SA convertion is unknown. (b) The content of SA in 14-d-old wild-type (WT) and *Osics1* mutants. (c) The content of SA in 14-d-old WT, *Osaim1* and complementation lines. 35S indicates complementation lines using 35S promoter, ProAIM1 indicates complementation lines using native promoter. (d) The relative content of BA in WT and *Osaim1* plants fed with 50 μM trans-cinnamic acid (CA) for 7 d. (e) The relative content of SA in WT and *Osaim1* plants fed with 50 μM CA for 7 d. (f) The relative content of SA in WT and *Osaim1* plants fed with 50 μM BA for 7 d. (g) The expression level of *OsAIM1* and *OsPR1b* in WT infected with *Xanthomonas oryzae* pv *Oryzae* (*Xoo*). (h) The relative content of SA in WT and *Osaim1* plants infected with *Xoo*. (i) The expression level of *OsICS1* in WT and *Osaim1* infected with *Xoo*. Error bars represent ± SD ($n = 3$ in b, c, f, g, h, i; $n = 4$ in d, e). Different letters show a significant difference by Tukey's test. Asterisks show a significant difference between CK and *Xoo* treatment (Student's *t*-test: **, $P < 0.005$; ***, $P < 0.001$). The plants were grown for 7 d and then subjected to chemical treatment for 7 d.

to SA. Consistent with a critical role of OsAIM1 in the β-oxidation of CA in the PAL pathway, the BA levels were also significantly reduced in the *Osaim1* mutant when compared with those in WT (Fig. 1d). To further confirm the role of OsAIM1 in SA biosynthesis, we performed chemical feeding experiments. Application with 50 μM CA resulted in a 1.4-fold increase in both BA and SA levels in WT plants (Fig. 1d,e). However, the same feeding treatment in the *Osaim1* mutant only slightly increased the BA levels and had no significant effect on the SA levels (Fig. 1d,e). By contrast, feeding with BA restored the SA content of *Osaim1* mutant to the WT levels (Fig. 1f). These results demonstrated that OsAIM1-mediated β-oxidation in the PAL pathway is required for the high basal levels of SA production in rice shoots.

Given that *Xanthomonas oryzae* pv *Oryzae* (*Xoo*) infection could increase SA production in rice (Bakade *et al.*, 2021), we also determined whether the OsAIM1-mediated β-oxidation is required for it. We first verify the expression of *OsAIM1* after *Xoo* (race PXO341) treatment. Similar to the positive control, *OsPR1b*, the expression of *OsAIM1* was induced by *Xoo* treatment (Fig. 1g). We further measured the SA levels in WT and *Osaim1* after *Xoo* treatment. It showed that the SA levels in WT

increased 2.5-fold after *Xoo* infection, whereas the SA levels in the *Osaim1* mutant were unchanged (Fig. 1h). Despite that the *Xoo* infection could not induce SA accumulation in the *Osaim1* mutant, it still induced the expression of *OsICS1* (Fig. 1i). It indicated that the *Xoo* induced SA biosynthesis was due to the OsAIM1-dependent pathway, other than the ICS pathway. Together, these results suggest that the OsAIM1-dependent pathway is not only crucial for basal SA biosynthesis, but also for pathogen-induced SA accumulation.

The high basal level of SA is required for modulating the steady-state stomatal aperture and shoot temperature

Rice shoots contain high basal levels of SA with little information on its biological function. In addition to its role in plant defense responses, SA is known to be important for heat production by inducing the expression of AOXs and promoting the alternative respiratory pathway in some thermogenic plants (Rhoads & McIntosh, 1992). To determine whether the high basal SA content influences the temperature of rice shoots, we took thermal images of WT and *Osaim1* mutant shoots by the infrared thermal camera. Consistently, we observed that the shoot temperature of the *Osaim1* mutant was over 1°C lower than that of WT (Fig. 2a,b). The decreased shoot temperature phenotype in *Osaim1* was completely rescued by the *OsAIM1* gene driven by the *CaMV 35S* or *OsAIM1* native promoter (Fig. 2a,b). To determine whether reduced SA content is responsible for the observed shoot temperature phenotype in the *Osaim1* mutant, we treated WT and *Osaim1* with SA. Exogenous SA application slightly increased the WT shoot temperature and could restore the shoot temperature of the *Osaim1* mutant to the WT level (Fig. 2c,d). To determine whether SA elevates rice shoot temperature through upregulating AOX genes as in some thermogenic plants, we compare the *AOX gene* expression between WT and the *Osaim1* mutant. qRT-PCR revealed that AOX gene expression was not compromised but was actually elevated in the *Osaim1* mutant when compared to that in WT (Fig. 2e). These findings indicated factors other than the AOX-based thermogenesis are responsible for reduced shoot temperature in the *Osaim1* mutant.

Transpiration also negatively influences leaf temperature (Lin *et al.*, 2017). Therefore, we examined the potential difference in transpiration between WT and the *Osaim1* mutant. Indeed, the *Osaim1* mutant displayed a transpiration rate *c.* 30% higher than WT (Fig. 2f). Consistent with increased transpiration, the detached leaves of the *Osaim1* mutant lost water more quickly than WT plants (Fig. S2a). Transpiration is mainly determined by stomata density, size, and aperture. However, we could not detect any significant difference in the density and size of stomata between WT and *Osaim1* mutant (Fig. S2b,c). Therefore, we further checked the stomatal apertures of the WT and *Osaim1* mutant using the scanning electron microscope. As shown in Fig. 2(g), there were higher percentages of completely open stomata in the *Osaim1* mutant (38%) than in WT (27%). The percentage of partially open stomata was *c.* 54% in WT and 58% in the *Osaim1* mutant (Fig. 2g). Consistent with the higher percentage of open stomata, the *Osaim1* mutant displayed higher stomatal conductance than WT (Fig. 2h).

Taken together, these results strongly suggest that the OsAIM1-dependent PAL pathway is responsible for the production of the high basal SA levels in rice shoots, which, in turn, is required for modulating stomatal aperture and transpiration to influence shoot temperature and other physiological traits.

SA regulates the stomatal aperture and shoot temperature through an OsWRKY45-dependent pathway

To determine how the high basal SA level regulates stomatal aperture and shoot temperature in rice, we analyzed the factors that are involved in SA signaling. Contrary to the central role of NPR1 in SA signaling in Arabidopsis, SA signaling in rice is mediated by both the OsNPR1 and OsWRKY45 sub-pathways (Shimono *et al.*, 2007; Nakayama *et al.*, 2013). To investigate the roles of OsNPR1 and OsWRKY45 in SA-regulated stomatal aperture and shoot temperature, we generated rice *Oswrky45* and *Osnpr1* loss-of-function mutants by CRISPR-Cas9 (Fig. S3). Like *Osaim1* mutant, the *Oswrky45* mutant displayed significantly lower shoot temperature than WT (Fig. 3a,b). Consistent with reduced shoot temperature, the *Oswrky45* mutant had an increased transpiration rate than WT plants (Fig. 3c). The detached leaves of the *Oswrky45* mutant also lost water more quickly than WT plants (Fig. S4). On the other hand, the shoot temperature, transpiration, and water loss rate of the *Osnpr1* mutant were all similar to those of WT (Figs 3a–c, S4). These results suggest that OsWRKY45, but not OsNPR1, mediates SA-regulated stomatal aperture and shoot temperatures. Consistent with this hypothesis, GUS staining of the $P_{OsWRKY45}$*:GUS* transgenic plant showed that *OsWRKY45* is highly expressed in the stomata apparatus (Fig. S5a), while expression of *OsNPR1* is absent in the stomata apparatus based on the histochemical staining of P_{OsNPR1}*:GUS* transgenic plants (Fig. S5b).

We further analyzed the stomatal apertures of the *Oswrky45* mutant and WT plants using scanning electron microscopy. As shown in Fig. 3(d), the percentage of completely open stomata in the *Oswrky45* mutant (29%) was significantly higher than that of WT (25%). The percentage of partially open stomata in the *Oswrky45* mutant (61%) was also significantly higher than that of WT (56%) (Fig. 3d). As a result, the percentage of completely closed stomata in the *Oswrky45* mutant (10%) was substantially lower than that of WT (19%; Fig. 3d). Consistent with the higher percentage of open stomata, the *Oswrky45* mutant also displayed higher stomatal conductance than WT (Fig. 3e). The decreased shoot temperature and increased stomatal conductance in *Oswrky45* were completely suppressed in the transgenic *Oswrky45* complementation lines containing the *OsWRKY45* genomic fragment (Fig. S6). These corroborate the role of *Os*WRKY45 in the modulation of stomatal aperture and shoot temperate in rice.

To further determine whether OsWRKY45 acts downstream of SA to regulate stomatal aperture and shoot temperatures, we analyzed the effect of SA on *OsWRKY45* expression. Both the qRT-PCR analysis and GUS staining analysis showed that

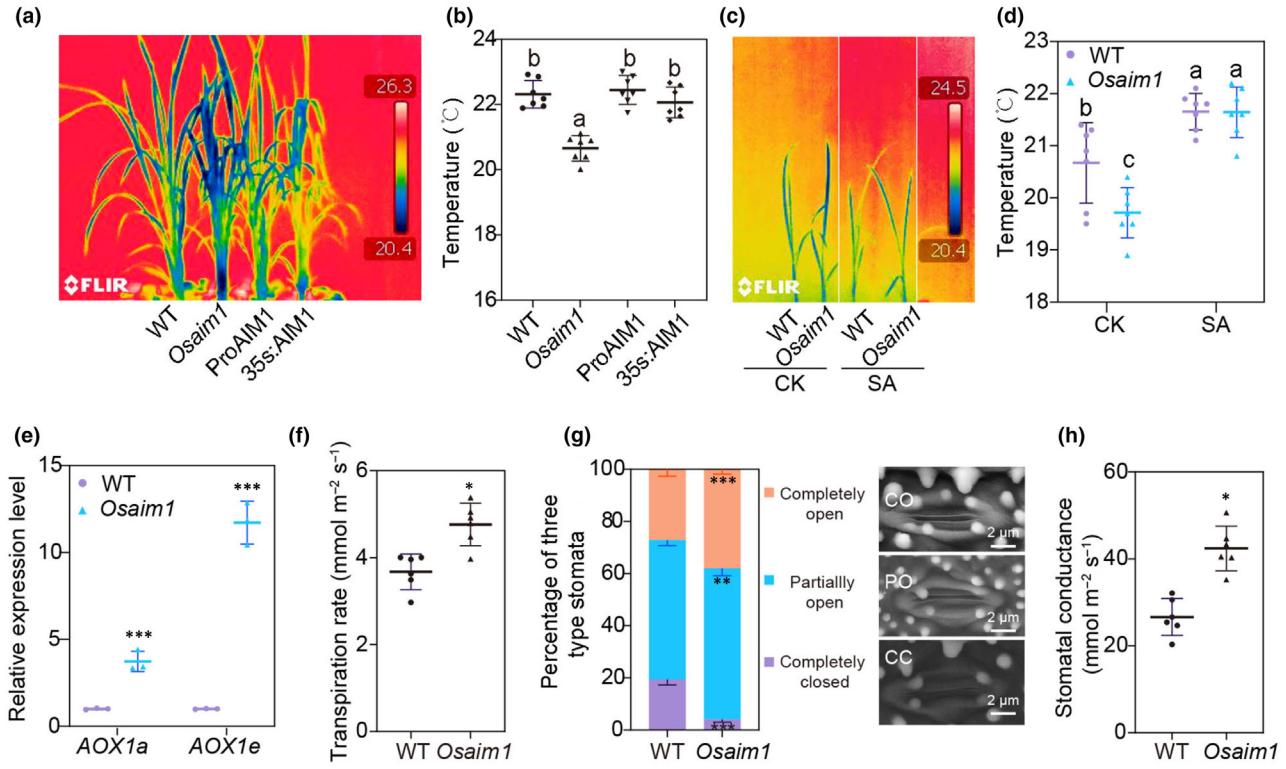

Fig. 2 OsAIM1 regulates stomatal aperture and shoot temperature in rice. (a) Infrared images of wild-type (WT), *Osaim1* and complementation lines. 35S indicates complementation lines using 35S promoter, ProAIM1 indicates complementation lines using native promoter. (b) Shoot temperature of WT, *Osaim1*, and complementation lines. (c) Infrared images of WT and *Osaim1* treated with or without salicylic acid (SA). (d) Temperature of WT and *Osaim1* treated with or without SA. (e) The expression level of *AOX1a* and *AOX1e* in WT and *Osaim1*. (f) Transpiration rate of WT and *Osaim1*. (g) Scanning electron microscopy images of three types of stomatal opening and the percentage of three types of stomatal opening in WT and *Osaim1*. CC, completely closed; CO, completely open; PO, partially open. (h) Stomatal conductance of WT and *Osaim1*. Error bars represent ± SD ($n = 7$ in b, $n = 3$ in e, $n = 6$ in d, f, h). Different letters show a significant difference by Tukey's test. Asterisks show a significant difference (Student's *t*-test: *, $P < 0.05$; **, $P < 0.01$; ***, $P < 0.001$ in e, f, h).

exogenous SA application strongly induced the expression of *OsWRKY45* in rice shoot and guard cells (Fig. 3f,g). To determine the effect of endogenous SA on *OsWRKY45* expression, we further analyzed the expression of *OsWRKY45* in the *Osaim1* mutant and found it to be significantly repressed in the mutant when compared with that in WT (Fig. 3f). The exogenous application of SA restored the expression of *OsWRKY45* in the *Osaim1* mutant to the WT level (Fig. 3f). By contrast, there was no significant alteration of *OsNPR1* expression in the *Osaim1* mutant relative to that in WT (Fig. S7). Given that SA treatment could rescue both *OsWRKY45* expression and the defects of stomatal apertures and shoot temperature in the *Osaim1* mutant, it is possible that the high basal SA level in rice shoots promotes *OsWRKY45* expression to regulate stomatal aperture, thereby affecting shoot temperature in rice. Reduced SA levels in the *Osaim1* mutant lead to increased stomatal aperture and reduced shoot temperature due to the reduction of *OsWRKY45* expression.

To test this possibility, we further generated the *Osaim1 Oswrky45* double mutant and compared the effects of SA on the single and double mutants. First, the *Osaim1 Oswrky45* double mutant had a shoot temperature similarly lower than WT as the *Osaim1* or *Oswrky45* single mutant (Fig. 3h,i). Thus, the effects of the *Osaim1* and *Oswrky45* mutations are not additive, supporting that they act in the same pathway. Second, unlike the *Osaim1* mutant, whose reduced shoot temperature could be restored by SA treatment, the *Oswrky45* single and *Osaim1 Oswrky45* double mutants were insensitive to SA application for restoration of their reduced shoot temperature (Fig. 3h,i). Likewise, while SA fully suppressed the elevated stomatal conductance of the *Osaim1* mutant, it failed to do so with the *Oswrky45* single and *Osaim1 Oswrky45* double mutants (Fig. 3e). The non-additive nature of the effects of the *Osaim1* and *Oswrky45* mutations and their differential responses to SA strongly support that OsWRKY45 acts downstream of the high basal shoot SA levels in the regulation of stomatal apertures and shoot temperatures in rice.

The high rice shoot basal SA maintains OsWRKY45 expression to affect H_2O_2 accumulation in the stomatal apparatus and promote abiotic stress tolerance

H_2O_2 is an important signaling molecule involved in the regulation of stomatal aperture (Waszczak *et al.*, 2018). Given the critical role of OsAIM1 and OsWRKY45 in the regulation of stomatal apertures, we further investigated the H_2O_2 levels in the

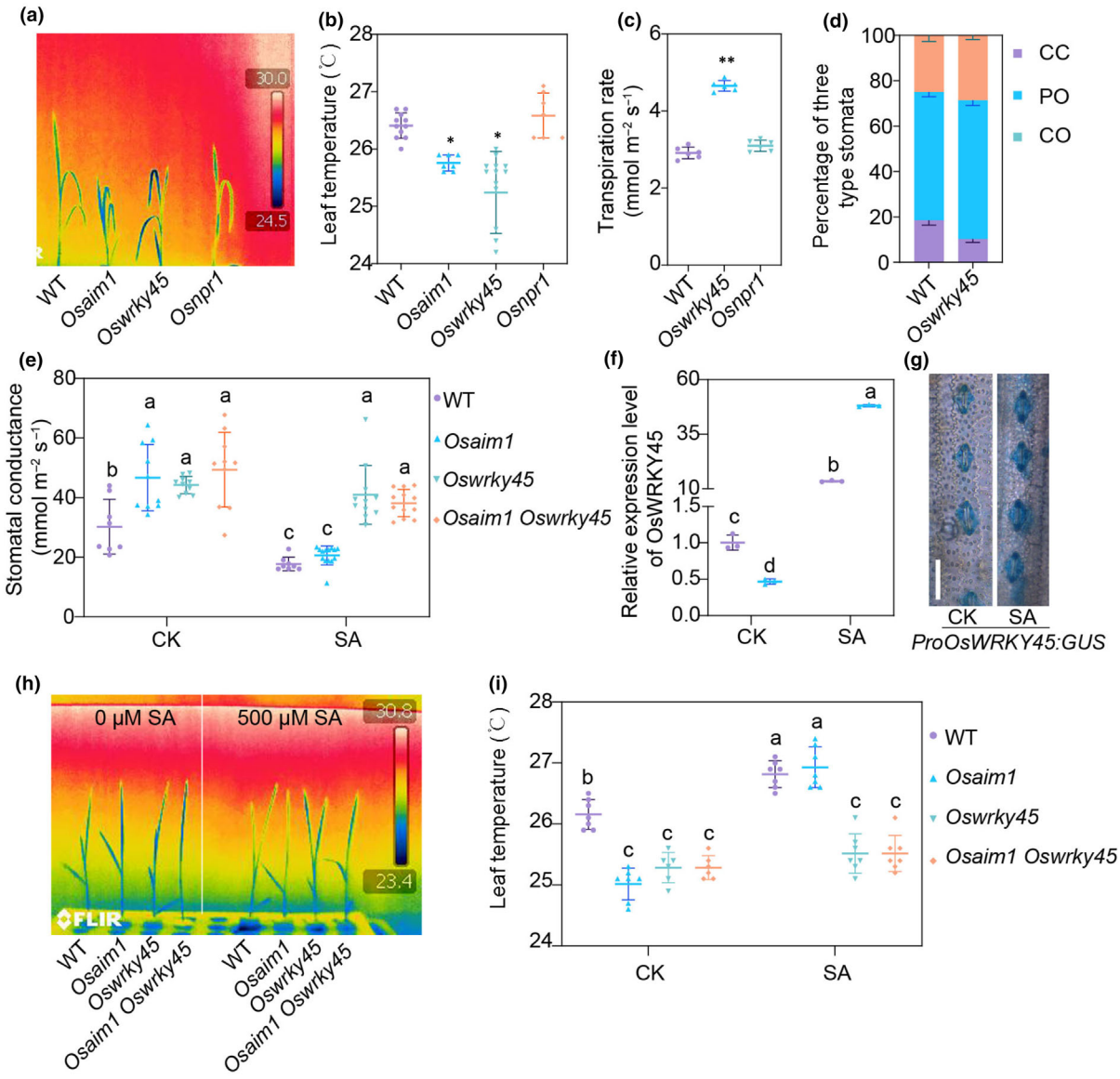

Fig. 3 Salicylic acid (SA) derived from OsAIM1 pathway regulate stomatal aperture and shoot temperature through OsWRKY45-dependent pathway in rice. (a) Infrared images of wild-type (WT), *Osaim1*, *Oswrky45*, and *Osnpr1* mutants. (b) Shoot temperature of WT, *Osaim1*, *Oswrky45*, and *Osnpr1* mutants. (c) Transpiration rate of WT and *Oswrky45*. (d) The percentage of three types of stomatal opening in WT and *Oswrky45*. CC, completely closed; CO, completely open; PO, partially open. (e) Stomatal conductance of WT, *Osaim1*, *Oswrky45*, and *Osaim1 wrky45* treated with or without SA. (f) The expression level of *WRKY45* WT and *Osaim1* treated with or without SA. (g) The expression of *ProWRKY45:GUS* in stomatal apparatus treated with or without SA treatment, Bar, 50 μm. (h) Infrared images of WT, *Osaim1*, *Oswrky45*, and *Osaim1 Oswrky45* double mutants treated with 0 or 500 μM SA. (i) Shoot temperature of WT, *Osaim1*, *Oswrky45* and *Osaim1 Oswrky45* double mutants treated with 0 or 500 μM SA. Error bars represent ± SD ($n = 7$ in b, $n = 5$ in c, $n = 9$ in e, $n = 3$ in f, $n = 7$ in i). Different letters show a significant difference by Tukey's test.

Osaim1 and *Oswrky45* mutants using 3′−ρ-HPF staining. Indeed, the H_2O_2 levels in the guard cells of the *Osaim1*, *Oswrky45*, and *Osaim1 Oswrky45* double mutants were decreased when compared to those in WT. To determine whether H_2O_2 is involved in OsWRKY45-regulated stomatal aperture, we also determined the effect of SA on the H_2O_2 levels in the guard cells of WT, *Osaim1*, *Oswrky45*, and *Osaim1 Oswrky45*. SA treatment stimulated H_2O_2 production in WT and could rescue the defect of reduced H_2O_2 accumulation in the *Osaim1* mutant, but not in the *Oswrky45* single and *Osaim1 Oswrky45* double mutants (Fig. 4a,b). Furthermore, the elevated stomatal conductance of the *Osaim1* and *Oswrky45* mutant was suppressed by H_2O_2 treatment (Fig. S8). These results indicate that the high basal SA level enhances H_2O_2 accumulation to regulate stomatal aperture in an OsWRKY45-dependent manner.

In rice, the DST zinc finger protein transcription factor interacts with another zinc finger protein DCA1 as a co-activator to affect drought and salt tolerance in rice via stomatal aperture control by regulating H_2O_2 homeostasis in rice (Huang *et al.*, 2009; Cui *et al.*, 2015). We analyzed the expression of *OsDST* and *OsDCA1* in both the *Osaim1* and *Oswrky45* mutants and found expression levels of both genes to be increased in the *Osaim1* and

Oswrky45 mutants (Fig. 4c). These results suggest that OsDCA1 and OsDST might participate in OsWRKY45-regulated H_2O_2 accumulation and stomatal aperture in rice.

Steady-state stomatal aperture is crucial for plant adaptation to abiotic stress (Cui *et al.*, 2015; Murata *et al.*, 2015; Sukiran *et al.*, 2020) and, therefore, the positive regulation of OsWRKY45 expression by the high basal shoot SA content could play a role in the plant tolerance to abiotic stress in rice. To test this, we first assessed the responses of WT and the *Osaim1* to salt and PEG treatments. Fourteen-day-old seedlings were first treated with 100 mM NaCl for 7 d or 20% PEG 6000 for 10 d and then recovered in the normal growth medium for 10 d. As shown in Fig. 4(d), the *Osaim1* mutant was substantially more sensitive to the salt and PEG treatments than WT. Approximately 40% and 70% of WT plants survived after the salt and PEG treatments, respectively (Fig. 4d–g). For comparison, only 8% and 24% of the *Osaim1* mutant plants survived under the salt and PEG treatments, respectively (Fig. 4d–g). Furthermore, exogenous application of SA could significantly increase the survival rate of *Osaim1* under the salt and PEG treatments. Thus, compromised SA synthesis resulted in hypersensitivity to salt and PEG treatments in the *Osaim1* mutant. Similar to the *Osaim1* mutant,

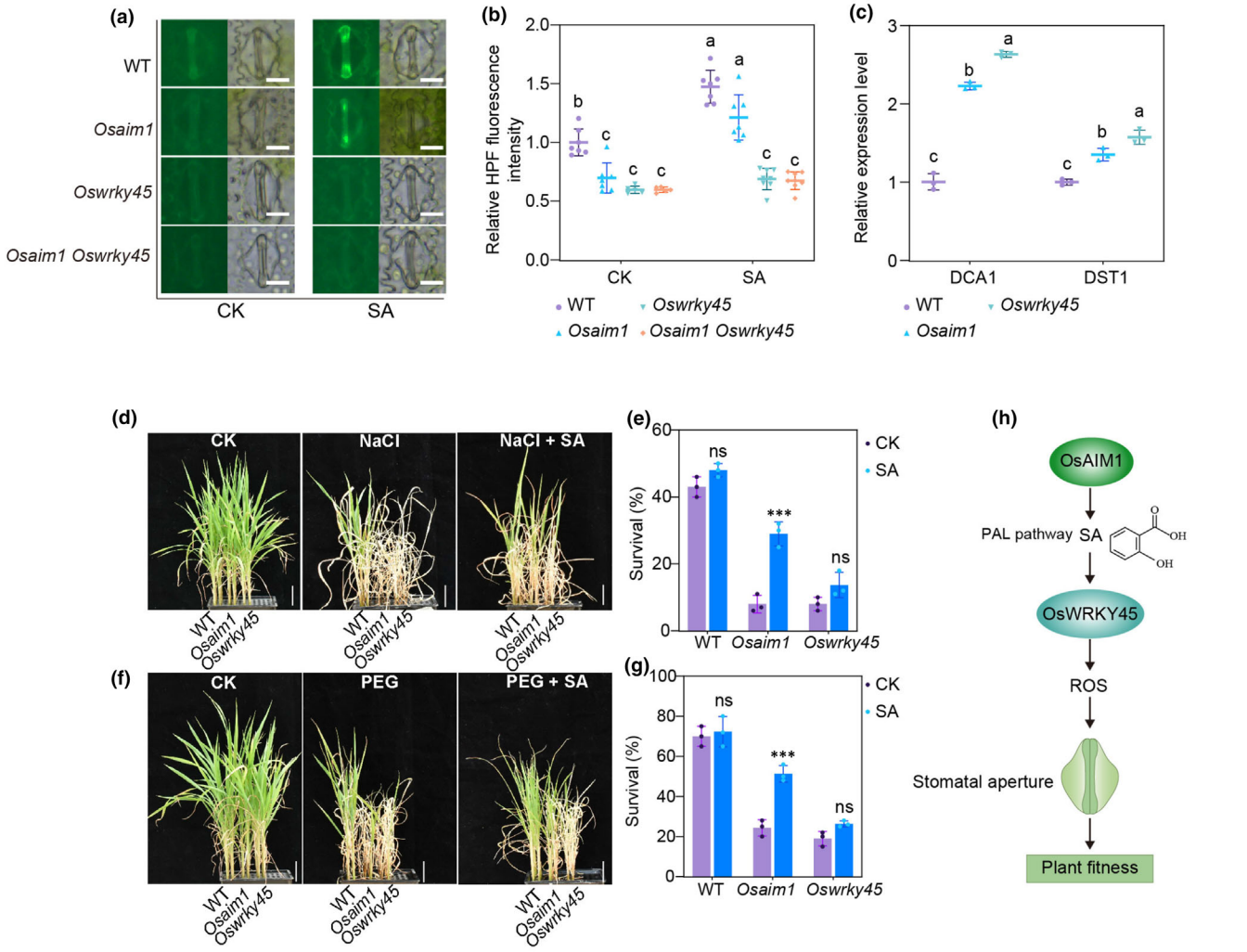

Fig. 4 Salicylic acid (SA) regulates reactive oxygen species (ROS) accumulation, stomatal aperture, and plant fitness in an OsWRKY45-dependent manner in rice. (a) Images of H_2O_2-based fluorescence signal in guard cells of 21-d-old seedlings of the wild-type (WT), *Osaim1*, *Oswrky45*, and *Osaim1 Oswrky45* double mutants, Bar, 10 μm. (b) The intensity of H_2O_2-based fluorescence signal in guard cells. The fluorescence intensity was quantified as the average pixel intensity of each guard cell using ImageJ. (c) The expression level of *DCA1* and *DST* in WT, *Osaim1* and *Oswrky45*. (d) Salt stress treatment of WT, *Osaim1*, and *Oswrky45* mutant. The 14-d-old seedlings were treated with 100 mM NaCl and 100 mM NaCl + 200 μM SA for 7 d (SA was added before NaCl treatment for 6 h) and then recovered for 10 d, Bar, 4 cm. (e) The survival rate of WT, *Osaim1*, and *Oswrky45* plants recovered for 7 d after NaCl treatment with or without SA treatment. (f) Polyethylene glycol (PEG) 6000 treatment of WT, *Osaim1*, and *Oswrky45* mutant. The 14-d-old seedlings were treated with 20% PEG and 20% PEG + 200 μM SA for 10 d (SA was added before PEG treatment for 6 h) and then recovered for 10 d, Bar, 4 cm. (g) The survival rate of WT, *Osaim1* and *Oswrky45* plants recovered for 7 d after PEG treatment with or without SA treatment. (h) A working model for the role of the OsWRKY45 mediated SA signaling in rice. SA was produced through OsAIM1-dependent phenylalanine ammonia-lyase (PAL) pathway in rice shoot. WRKY45-ROS acts downstream of SA to regulate stomatal aperture and abiotic stress response. Error bars represent ± SD ($n = 7$ in b, $n = 3$ in c, e, g). Different letters show a significant difference by Tukey's test. Asterisks show a significant difference (Student's *t*-test: ***, $P < 0.001$). ns, not significant, HPF, 3′-(p-hydroxyphenyl) fluorescein.

the *Oswrky45* mutant was less tolerant to both the salt and PEG treatments. However, SA application failed to restore the tolerance to salt and PEG treatments in the *Oswrky45* mutant (Fig. 4d–g). After salt and PEG treatments, the *Osaim1* and *Oswrky45* mutants still displayed lower H_2O_2 levels and higher stomatal conductance compared with WT. However, SA application could rescue the defects of H_2O_2 accumulation and stomatal conductance of *Osaim1*, but not *Oswrky45* under salt and PEG treatments (Fig. S9).

Taken all these results together, OsAIM1-dependent PAL pathway is essential for the accumulation of high basal level SA in rice shoots. In addition, the high basal level of SA is required for the regulation of the steady-state stomatal aperture through an OsWRKY45-dependent pathway in rice, which is crucial for abiotic stress tolerance in the important crop (Fig. 4h).

Discussion

Salicylic acid acts as a signaling molecule in plant inducible responses against various forms of environmental stresses and its biosynthesis is stress responsive in many plant species. Salicylic acid can be synthesized through two distinct pathways in plants, the ICS pathway and the PAL pathway (Ding & Ding, 2020). Isochorismate synthase plays an important role in SA production in some plant species (Rekhter *et al.*, 2019). In *Arabidopsis thaliana*, *AtICS1* is essential for stress-induced SA production. Likewise, a *Nicotiana benthamiana* ICS gene (*NbICS*) is transcriptionally induced by a pathogen elicitor and is required for induced SA production in response to biotic and abiotic stress conditions (Catinot *et al.*, 2008; Shibata *et al.*, 2010). By contrast, ICS in tobacco (*Nicotiana tabacum*; *NtICS*) does not appear to be involved in stress-induced SA production. The transcript levels of *NtICS* were not induced, and ICS activity was undetectable when SA production was induced by tobacco mosaic virus inoculation or ozone exposure (Ogawa *et al.*, 2005). Rice constitutively contains two to three orders of magnitude higher levels of SA than *Arabidopsis*, *N. benthamiana*, and tobacco. If OsICS is required for the production of such higher levels of SA in rice, its activity would be expected to be much higher than that of AtICS1, NbICS, and NtICS. However, a recent study has shown that the *in vitro* and *in planta* ICS activities of OsICS were much lower than those of AtICS1 (Yokoo *et al.*, 2018). Previously, we have found that OsAIM1-dependent β-oxidation is required for SA biosynthesis in rice roots (Xu *et al.*, 2017). A recent study found that AIM1-dependent β-oxidation is required for the biosynthesis of SA in chlorophyte algae (Jia *et al.*, 2023). In this study, we have further found that OsAIM1 is crucial for the biosynthesis of high levels of basal SA in rice shoots. The basal SA level in the shoots of rice *Osaim1* mutant was reduced by almost 90% when compared with that in WT shoots. Thus, OsAIM1-dependent β-oxidation in the PAL pathway is responsible for the synthesis of a majority of basal SA in rice. Meanwhile, OsAIM1 is also required for pathogen induced SA biosynthesis. Although the ICS1 is present in the rice, our results indicate that it does not participate in the biosynthesis of high levels of basal SA. Therefore, the biosynthesis pathway of SA may vary in different plants. However, we could not exclude the possibility that ICS is responsible for SA biosynthesis in certain stress conditions in rice.

In Arabidopsis, most pathogen-induced SA is derived from isochorismate, which is generated from chorismate by ICS1 in the plastid (Rekhter *et al.*, 2019). Isochorismate generated by ICS is also an early precursor for phylloquinone, which can be synthesized via 1,4-dihydroxy-2-naphthoic acid (DHNA) in a multistep pathway (Gross *et al.*, 2006). As a result, Arabidopsis *ics1 ics2* double mutant is deficient not only in SA but also in phylloquinone biosynthesis. Because phylloquinone is essential for electron transfer in photosystem I, the *ics1 ics2* double mutants are smaller than WT and display chlorosis (Garcion *et al.*, 2008). Like rice, barley contains a single ICS gene. Phylloquinone in the barley *ics1* mutant is undetectable and the mutant displays wilting symptoms, both of these phenotypes could be rescued by DHNA application, indicating that the wilting phenotype of barley *ics1* mutant is caused by phylloquinone deficiency (Qin *et al.*, 2019). However, the SA level in barley *ics1* mutant was comparable to that in WT. Similarly, we have found that the SA content in the *Osics1* mutant was similar to that of WT. These results indicate that OsICS1 might be required for the production of phylloquinone but not SA in rice.

Rice shoot accumulates an extremely high basal level of SA, almost 100-fold higher than that in Arabidopsis. A previous report has found that SA plays an important role in protecting rice from oxidative damage (Yang *et al.*, 2004). Here, we found that the high basal SA level in rice shoot is required for the maintenance of shoot temperatures by modulating the stomatal aperture. The *Osaim1* mutant had *c.* 90% less SA than WT in shoot and displayed increased stomatal aperture and reduced shoot temperatures relative to those in WT. NPR1 is the master regulator of SA-mediated responses (Dong, 2004), and SA induces stomatal closure in an NPR1-dependent manner in Arabidopsis (Ou *et al.*, 2022). In rice, however, both OsNPR1 and OsWRKY45 play a crucial role in SA signaling (Shimono *et al.*, 2007). Our results demonstrate that an OsWRKY45, rather than OsNPR1, plays a critical role in SA-regulated stomatal aperture. H_2O_2 is an important signal molecule that induces stomatal closure (Waszczak *et al.*, 2018). We have found that OsWRKY45-dependent SA signaling pathway may control stomata aperture by regulating H_2O_2 accumulation. H_2O_2 level was decreased in the *Osaim1*, *Oswrky45* single and *Osaim1 Oswrky45* double mutants. Salicylic acid treatment could rescue the H_2O_2 accumulation defect of *Osaim1*, but not the *Oswrky45* and *Osaim1 Oswrky45* mutants, suggesting that OsWRKY45 acts downstream of SA to regulate H_2O_2 accumulation in rice. Furthermore, we found that the expression of *OsDCA1* and *OsDST*, negative regulators of stomatal closure via regulating H_2O_2 homeostasis, increased in the *Osaim1* and *Oswrky45* mutants. These results suggest that the high basal SA level in rice shoot may maintain the steady-state stomatal aperture through OsWRKY45-H_2O_2 signaling pathway.

In addition to its crucial role in plant biotic stress response, SA plays an important role in plant response to abiotic stresses, such as salt, drought, and cold (Rivas-San Vicente & Plasencia, 2011). Although many studies have analyzed the effect of SA on abiotic stresses in plants, its role and molecular mechanism in abiotic

stress tolerance in rice are still poorly understood. Steady-state stomatal aperture is a key component in plant adaption to abiotic stress (Cui *et al.*, 2015; Murata *et al.*, 2015; Sukiran *et al.*, 2020). Therefore, the high basal SA level in rice shoots may maintain the steady-state stomatal aperture to increase the abiotic stress tolerance. Indeed, we have found that *Osaim1* and *Oswrky45* are more sensitive to NaCl and PEG treatment, and exogenous SA could restore this phenotype of *Osaim1*, but not *Oswrky45*. These results support that steady-state stomatal aperture maintained by the OsWRKY45-dependent SA signaling pathway is crucial for abiotic stress tolerance in rice. As sessile organisms constantly exposed to diverse environmental challenges, including biotic and abiotic stress, plants have evolved complex molecular mechanisms to increase their adaptation and fitness. In this study, we have established that OsWRKY45 is a key player in SA-mediated abiotic stress adaptation. Previous studies have found that OsWRKY45 plays a crucial role in SA-mediated defense signaling by activating redox-related genes in rice (Shimono *et al.*, 2007). Regulation of stomatal aperture also contributes to plant defense by restricting pathogen entry into plants (Melotto *et al.*, 2008). Thus, OsWRKY45 is a critical regulator of stomatal closure in the SA signaling pathway in plant responses to both biotic and abiotic stresses.

In summary, we have shown here that the OsAIM1-dependent PAL pathway is essential for the biosynthesis of high basal levels of SA in rice shoot. We have also found that the high basal SA level in rice shoot is required for maintaining the steady-state stomatal aperture through an OsWRKY45-dependent pathway, which is important for enhanced plant tolerance to abiotic stresses.

Acknowledgements

This work was supported by the National Natural Science Foundation (32130096, 31800246), the Youth innovation Program of Chinese Academy of Agricultural Sciences (no. Y2022QC14), and Natural Science Foundation of Tianjin (20JCYBJC00260). KY was supported by the Agricultural Science and Technology Innovation Program of Chinese Academy of Agricultural Sciences.

Competing interests

None declared.

Author contributions

KY, LX, XX and JL conceived the project and designed the research. LX, HZ, JW, XW, XJ, LW, ZX and RL performed the experiments. LX, HZ, KJ, ZC, JL, XX and KY were involved in analyzing the data and preparing the manuscript. LX, HZ and JW contributed equally to this work.

ORCID

Xianqing Jia https://orcid.org/0000-0003-2033-2048
Kun Jiang https://orcid.org/0000-0002-8199-9164
Jie Luo https://orcid.org/0000-0001-9508-4494
Junbin Wang https://orcid.org/0000-0001-9728-780X
Long Wang https://orcid.org/0000-0001-8123-6071
Xuming Wang https://orcid.org/0000-0002-6303-2371
Xiaodong Xie https://orcid.org/0000-0001-8434-8423
Lei Xu https://orcid.org/0000-0003-4157-0686
Keke Yi https://orcid.org/0000-0002-3916-477X
Hongyu Zhao https://orcid.org/0000-0003-4744-0153

Data availability

The data that support the findings of this study are available from the corresponding author upon reasonable request.

References

Bakade R, Ingole KD, Deshpande S, Pal G, Patil SS, Bhattacharjee S, Prasannakumar MK, Ramu VS. 2021. Comparative transcriptome analysis of rice resistant and susceptible genotypes to *Xanthomonas oryzae* pv *oryzae* identifies novel genes to control bacterial leaf blight. *Molecular Biotechnology* **63**: 719–731.

Bussell JD, Reichelt M, Wiszniewski AA, Gershenzon J, Smith SM. 2014. Peroxisomal ATP-binding cassette transporter COMATOSE and the multifunctional protein abnormal INFLORESCENCE MERISTEM are required for the production of benzoylated metabolites in Arabidopsis seeds. *Plant Physiology* **164**: 48–54.

Catinot J, Buchala A, Abou-Mansour E, Metraux JP. 2008. Salicylic acid production in response to biotic and abiotic stress depends on isochorismate in *Nicotiana benthamiana*. *FEBS Letters* **582**: 473–478.

Chen W, Gong L, Guo Z, Wang W, Zhang H, Liu X, Yu S, Xiong L, Luo J. 2013. A novel integrated method for large-scale detection, identification, and quantification of widely targeted metabolites: application in the study of rice metabolomics. *Molecular Plant* **6**: 1769–1780.

Choi C, Hwang SH, Fang IR, Kwon SI, Park SR, Ahn I, Kim JB, Hwang DJ. 2015. Molecular characterization of *Oryza sativa* WRKY6, which binds to W-box-like element 1 of the *Oryza sativa* pathogenesis-related (PR) 10a promoter and confers reduced susceptibility to pathogens. *New Phytologist* **208**: 846–859.

Cui LG, Shan JX, Shi M, Gao JP, Lin HX. 2015. DCA1 acts as a transcriptional co-activator of DST and contributes to drought and salt tolerance in rice. *PLoS Genetics* **11**: e1005617.

Dempsey DA, Vlot AC, Wildermuth MC, Klessig DF. 2011. Salicylic acid biosynthesis and metabolism. *Arabidopsis Book* **9**: e0156.

Ding P, Ding Y. 2020. Stories of salicylic acid: a plant defense hormone. *Trends in Plant Science* **25**: 549–565.

Dong X. 2004. NPR1, all things considered. *Current Opinion in Plant Biology* **7**: 547–552.

Garcion C, Lohmann A, Lamodiere E, Catinot J, Buchala A, Doermann P, Metraux JP. 2008. Characterization and biological function of the *ISOCHORISMATE SYNTHASE2* gene of Arabidopsis. *Plant Physiology* **147**: 1279–1287.

Gross J, Cho WK, Lezhneva L, Falk J, Krupinska K, Shinozaki K, Seki M, Herrmann RG, Meurer J. 2006. A plant locus essential for phylloquinone (vitamin K1) biosynthesis originated from a fusion of four eubacterial genes. *The Journal of Biological Chemistry* **281**: 17189–17196.

Huang XY, Chao DY, Gao JP, Zhu MZ, Shi M, Lin HX. 2009. A previously unknown zinc finger protein, DST, regulates drought and salt tolerance in rice via stomatal aperture control. *Genes & Development* **23**: 1805–1817.

Jia X, Wang L, Zhao H, Zhang Y, Chen Z, Xu L, Yi K. 2023. The origin and evolution of salicylic acid signaling and biosynthesis in plants. *Molecular Plant* **16**: 245–259.

Jiang G, Yin D, Shi Y, Zhou Z, Li C, Liu P, Jia Y, Wang Y, Liu Z, Yu M *et al.* 2020. OsNPR3.3-dependent salicylic acid signaling is involved in recessive gene xa5-mediated immunity to rice bacterial blight. *Scientific Reports* **10**: 6313.

Kouzai Y, Kimura M, Watanabe M, Kusunoki K, Osaka D, Suzuki T, Matsui H, Yamamoto M, Ichinose Y, Toyoda K *et al.* 2018. Salicylic acid-dependent

immunity contributes to resistance against *Rhizoctonia solani*, a necrotrophic fungal agent of sheath blight, in rice and *Brachypodium distachyon*. *New Phytologist* **217**: 771–783.

Lin H, Chen YJ, Zhang HL, Fu PL, Fan ZX. 2017. Stronger cooling effects of transpiration and leaf physical traits of plants from a hot dry habitat than from a hot wet habitat. *Functional Ecology* **31**: 2202–2211.

Melotto M, Underwood W, He SY. 2008. Role of stomata in plant innate immunity and foliar bacterial diseases. *Annual Review of Phytopathology* **46**: 101–122.

Murata Y, Mori IC, Munemasa S. 2015. Diverse stomatal signaling and the signal integration mechanism. *Annual Review of Plant Biology* **66**: 369–392.

Nakayama A, Fukushima S, Goto S, Matsushita A, Shimono M, Sugano S, Jiang CJ, Akagi A, Yamazaki M, Inoue H *et al.* 2013. Genome-wide identification of WRKY45-regulated genes that mediate benzothiadiazole-induced defense responses in rice. *BMC Plant Biology* **13**: 150.

Ogawa D, Nakajima N, Sano T, Tamaoki M, Aono M, Kubo A, Kanna M, Ioki M, Kamada H, Saji H. 2005. Salicylic acid accumulation under O_3 exposure is regulated by ethylene in tobacco plants. *Plant & Cell Physiology* **46**: 1062–1072.

Ou X, Li T, Zhao Y, Chang Y, Wu L, Chen G, Day B, Jiang K. 2022. Calcium-dependent ABA signaling functions in stomatal immunity by regulating rapid SA responses in guard cells. *Journal of Plant Physiology* **268**: 153585.

Pal M, Kovacs V, Szalai G, Soos V, Ma X, Liu H, Mei H, Janda T. 2014. Salicylic acid and abiotic stress responses in rice. *Journal of Agronomy and Crop Science* **200**: 1–11.

Qin Y, Torp AM, Glauser G, Pedersen C, Rasmussen SK, Thordal-Christensen H. 2019. Barley isochorismate synthase mutant is phylloquinone-deficient, but has normal basal salicylic acid level. *Plant Signaling & Behavior* **14**: 1671122.

Raskin I. 1992. Salicylate, a new plant hormone. *Plant Physiology* **99**: 799–803.

Raskin I, Ehmann A, Melander WR, Meeuse BJ. 1987. Salicylic acid: a natural inducer of heat production in arum lilies. *Science* **237**: 1601–1602.

Raskin I, Turner IM, Melander WR. 1989. Regulation of heat production in the inflorescences of an *Arum* lily by endogenous salicylic acid. *Proceedings of the National Academy of Sciences, USA* **86**: 2214–2218.

Rekhter D, Ludke D, Ding Y, Feussner K, Zienkiewicz K, Lipka V, Wiermer M, Zhang Y, Feussner I. 2019. Isochorismate-derived biosynthesis of the plant stress hormone salicylic acid. *Science* **365**: 498–502.

Rhoads DM, McIntosh L. 1992. Salicylic acid regulation of respiration in higher plants: alternative oxidase expression. *Plant Cell* **4**: 1131–1139.

Rivas-San Vicente M, Plasencia J. 2011. Salicylic acid beyond defence: its role in plant growth and development. *Journal of Experimental Botany* **62**: 3321–3338.

Shibata Y, Kawakita K, Takemoto D. 2010. Age-related resistance of *Nicotiana benthamiana* against hemibiotrophic pathogen *Phytophthora infestans* requires both ethylene- and salicylic acid-mediated signaling pathways. *Molecular Plant–Microbe Interactions* **23**: 1130–1142.

Shimono M, Sugano S, Nakayama A, Jiang CJ, Ono K, Toki S, Takatsuji H. 2007. Rice WRKY45 plays a crucial role in benzothiadiazole-inducible blast resistance. *Plant Cell* **19**: 2064–2076.

Shine MB, Yang JW, El-Habbak M, Nagyabhyru P, Fu DQ, Navarre D, Ghabrial S, Kachroo P, Kachroo A. 2016. Cooperative functioning between phenylalanine ammonia lyase and isochorismate synthase activities contributes to salicylic acid biosynthesis in soybean. *New Phytologist* **212**: 627–636.

Silverman P, Seskar M, Kanter D, Schweizer P, Metraux JP, Raskin I. 1995. Salicylic acid in rice (biosynthesis, conjugation, and possible role). *Plant Physiology* **108**: 633–639.

Sukiran NA, Steel PG, Knight MR. 2020. Basal stomatal aperture is regulated by GA-DELLAs in Arabidopsis. *Journal of Plant Physiology* **250**: 153182.

Tan S, Abas M, Verstraeten I, Glanc M, Molnar G, Hajny J, Lasak P, Petrik I, Russinova E, Petrasek J *et al.* 2020. Salicylic acid targets protein phosphatase 2A to attenuate growth in plants. *Current Biology* **30**: 381–395.

Waszczak C, Carmody M, Kangasjarvi J. 2018. Reactive oxygen species in plant signaling. *Annual Review of Plant Biology* **69**: 209–236.

White RF. 1979. Acetylsalicylic acid (aspirin) induces resistance to tobacco mosaic virus in tobacco. *Virology* **99**: 410–412.

Wildermuth MC, Dewdney J, Wu G, Ausubel FM. 2001. Isochorismate synthase is required to synthesize salicylic acid for plant defence. *Nature* **414**: 562–565.

Xu L, Zhao H, Ruan W, Deng M, Wang F, Peng J, Luo J, Chen Z, Yi K. 2017. ABNORMAL INFLORESCENCE MERISTEM1 functions in salicylic acid biosynthesis to maintain proper reactive oxygen species levels for root meristem activity in rice. *Plant Cell* **29**: 560–574.

Xue LJ, Guo W, Yuan Y, Anino EO, Nyamdari B, Wilson MC, Frost CJ, Chen HY, Babst BA, Harding SA *et al.* 2013. Constitutively elevated salicylic acid levels alter photosynthesis and oxidative state but not growth in transgenic populus. *Plant Cell* **25**: 2714–2730.

Yang Y, Qi M, Mei C. 2004. Endogenous salicylic acid protects rice plants from oxidative damage caused by aging as well as biotic and abiotic stress. *The Plant Journal* **40**: 909–919.

Yokoo S, Inoue S, Suzuki N, Amakawa N, Matsui H, Nakagami H, Takahashi A, Arai R, Katou S. 2018. Comparative analysis of plant isochorismate synthases reveals structural mechanisms underlying their distinct biochemical properties. *Bioscience Reports* **38**: BSR20171457.

Yuan Y, Chung JD, Fu X, Johnson VE, Ranjan P, Booth SL, Harding SA, Tsai CJ. 2009. Alternative splicing and gene duplication differentially shaped the regulation of isochorismate synthase in *Populus* and *Arabidopsis*. *Proceedings of the National Academy of Sciences, USA* **106**: 22020–22025.

Zhang K, Halitschke R, Yin C, Liu CJ, Gan SS. 2013. Salicylic acid 3-hydroxylase regulates *Arabidopsis* leaf longevity by mediating salicylic acid catabolism. *Proceedings of the National Academy of Sciences, USA* **110**: 14807–14812.

Supporting Information

Additional Supporting Information may be found online in the Supporting Information section at the end of the article.

Fig. S1 Characterization of *Osics1* mutant.

Fig. S2 Water loss, stomata density, and size of wild-type and *Osaim1*.

Fig. S3 Sequence information of *NPR1* and *WRKY45* in their mutants.

Fig. S4 Water loss of detached leaves of wild-type, *Oswrky45*, and *Osnpr1*.

Fig. S5 The expression of *ProWRKY45:GUS* and *ProNPR1:GUS* in leaf.

Fig. S6 Phenotype of wild-type, *Oswrky45* mutant, and *Oswrky45* complementation lines.

Fig. S7 The expression level of *NPR1* in wild-type and *Osaim1*.

Fig. S8 The elevated stomatal conductance of the *Osaim1* and *Oswrky45* mutant was suppressed by H_2O_2 treatment.

Fig. S9 The H_2O_2 levels and stomatal conductance of wild-type, *Osaim1*, and *Oswrky45* plants under different conditions.

Table S1 Primer used in this study.

Please note: Wiley is not responsible for the content or functionality of any Supporting Information supplied by the authors. Any queries (other than missing material) should be directed to the *New Phytologist* Central Office.